Molecules **2014**, *19*, 17279-17304; doi:10.3390/molecules191117279

OPEN ACCESS

molecules

ISSN 1420-3049

www.mdpi.com/journal/molecules

Article

Radical Intermediates in Photoinduced Reactions on TiO_2 (An EPR Spin Trapping Study)

Dana Dvoranová, Zuzana Barbieriková and Vlasta Brezová *

Institute of Physical Chemistry and Chemical Physics, Faculty of Chemical and Food Technology, Slovak University of Technology in Bratislava, Radlinského 9, Bratislava SK-812 37, Slovakia

* Author to whom correspondence should be addressed; E-Mail: vlasta.brezova@stuba.sk; Tel.: +421-259-325-666; Fax: +421-259-325-751.

External Editor: Pierre Pichat

Received: 13 August 2014; in revised form: 29 September 2014 / Accepted: 22 October 2014 / Published: 28 October 2014

Abstract: The radical intermediates formed upon UVA irradiation of titanium dioxide suspensions in aqueous and non-aqueous environments were investigated applying the EPR spin trapping technique. The results showed that the generation of reactive species and their consecutive reactions are influenced by the solvent properties (e.g., polarity, solubility of molecular oxygen, rate constant for the reaction of hydroxyl radicals with the solvent). The formation of hydroxyl radicals, evidenced as the corresponding spin-adducts, dominated in the irradiated TiO_2 aqueous suspensions. The addition of ^{17}O-enriched water caused changes in the EPR spectra reflecting the interaction of an unpaired electron with the ^{17}O nucleus. The photoexcitation of TiO_2 in non-aqueous solvents (dimethylsulfoxide, acetonitrile, methanol and ethanol) in the presence of 5,5-dimethyl-1-pyrroline *N*-oxide spin trap displayed a stabilization of the superoxide radical anions generated via electron transfer reaction to molecular oxygen, and various oxygen- and carbon-centered radicals from the solvents were generated. The character and origin of the carbon-centered spin-adducts was confirmed using nitroso spin trapping agents.

Keywords: titanium dioxide; hydroxyl radical; reactive oxygen species; EPR spectroscopy; spin trapping technique; sterically hindered amines

---

1. Introduction

Among the materials previously studied as potential photocatalysts, titanium dioxide meets the criteria for industrial-scale utilization. Stability, low cost, relatively low toxicity and appropriate photocatalytic activity predispose TiO_2 to a wide range of applications in various areas (gas sensors, photocatalysts, solar cells, thin film capacitors, self-cleaning surfaces, *etc.*) [1–6]. Especially attractive are nowadays the prospects of titania photocatalysts applications in the remediation of polluted water, soil and air, or in unconventional organic syntheses [7–13]. Consequently, all titanium dioxide polymorphs (anatase, brookite, rutile) have been intensively studied regarding their ability to produce, upon UVA photoexcitation, electron (e^-) and hole (h^+) pairs further involved in the consecutive chemical reactions [1,2,5,14–16]. In general, the photoactivity of TiO_2 is determined by the processes of electron/hole pair generation, recombination, interfacial transfer and by the surface reactions of these charge carriers with the species adsorbed on the surface of the photocatalyst [1,2,5,10,15–17]. The photoinduced processes on TiO_2 nanoparticles upon ultra-band gap irradiation are also well influenced by the bulk structure, surface properties and the electronic structure of the photocatalyst [5]. The reactions of photogenerated holes with the adsorbed hydroxide anions and water molecules lead to the formation of highly reactive hydroxyl radicals, which, together with the hole itself, can initiate the oxidative degradation of organic pollutants down to water and carbon dioxide [1,2,5,10,16]. The efficient production of hydroxyl radicals and their non-selective reactions with organic and inorganic pollutants represent a crucial point considering the application of photocatalytic processes in water and air purification [1]. Recent investigations have revealed different mechanisms on anatase and rutile surfaces [18], as well as the role of surface-bridging oxygens of TiO_2 on the $^{\bullet}OH$ formation associated with the oxidation of surface hydroxide anions and water molecules by the photogenerated holes [19,20]. The presence of molecular oxygen also plays a substantial role in the photoinduced processes on irradiated TiO_2 surfaces, as it enables an effective charge carriers separation. The electrons trapped transiently on the surface or on the next-to-surface defects can react with the adsorbed oxygen molecules [21–23]. The consecutive reactions of the so generated $O_2^{\bullet-}$ are influenced by the solvent properties [24]. Although the superoxide radical anion is quite stable in the aprotic solvents [25], in aqueous solutions the reaction with protons is favorable, and hydrogen peroxide is formed and involved in further photocatalytic processes, Equations (1)–(6) [26]:

$$O_2^{\bullet-} + H^+ \rightarrow {}^{\bullet}O_2H \quad (1)$$

$$2\ {}^{\bullet}O_2H \rightarrow H_2O_2 + O_2 \quad (2)$$

$$H_2O_2 + O_2^{\bullet-} \rightarrow {}^{\bullet}OH + O_2 + OH^- \quad (3)$$

$$H_2O_2 \xrightarrow{h\nu} 2\ {}^{\bullet}OH \quad (4)$$

$$H_2O_2 + e^- \rightarrow {}^{\bullet}OH + OH^- \quad (5)$$

$$H_2O_2 + h^+ + OH^- \rightarrow H_2O + {}^{\bullet}O_2H \quad (6)$$

Consequently, superoxide radical anion and hydrogen peroxide as the most important products of the molecular oxygen reduction play an important role in the complex mechanism of Reactive

Oxygen Species (ROS, e.g., $^{\bullet}OH$, $^{\bullet}O_2H$ or singlet oxygen) generation on the irradiated TiO_2 surfaces [1,18,26–28].

EPR spectroscopy occupies an exclusive position in the investigation of titania photocatalysts, providing a characterization of paramagnetic centers produced via the trapped photogenerated electrons and holes [29–36], and of titanium dioxide materials with transition-metal ions doping [17,34]. A majority of the research exploiting EPR spectroscopy deals with the investigation of reactive radical intermediates produced in the irradiated TiO_2 particulate systems where the application of an indirect spin trapping technique is inevitable [37–45]. This method is based on the chemical reaction of a diamagnetic spin trap (ST) with a short-lived radical, producing a more stable nitroxide radical, *i.e.*, spin-adduct, using nitrones, *N*-oxides and nitroso compounds as the spin trapping agents (Figure 1). Spin traps possessing *N*-oxide and nitrone groups are mainly applied in the identification of hydroxyl radicals generation, as well as other oxygen-, nitrogen- and sulfur-centered reactive radicals, however the information on the structure of carbon-centered radicals trapped with these agents is limited, and the application of nitroso spin traps is necessary to bring the knowledge on other nuclei in the vicinity of the trapped carbon [46,47]. Successful assignment of measured EPR spectra of spin-adducts requires a thorough interpretation of the acquired data and careful choice of the spin trapping agent for the specific experimental conditions [48].

Figure 1. Overview of the spin trapping agents applied in *in situ* EPR investigations.

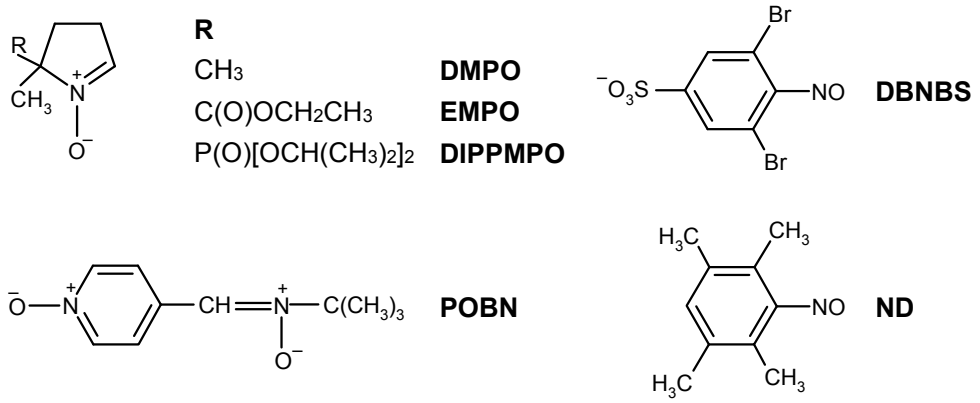

In the literature hydroxyl radicals are frequently declared as the most important reactive species generated upon TiO_2 irradiation, in spite of the addition of organic co-solvent to the reaction systems, which effects the character and amount of radicals formed. The main aim of our study was to point on the formation of radical intermediates in aqueous TiO_2 suspensions, as well as in suspensions prepared in an organic solvent (DMSO, acetonitrile, methanol, ethanol) and thus provide a straightforward comparison of the radical species detected under UVA exposure of TiO_2 suspended in water and in aprotic and protic polar solvents exploiting the *in situ* EPR spin trapping technique. The oxidation of sterically hindered amines to the corresponding nitroxide radicals via ROS photogenerated in the aqueous and acetonitrile TiO_2 suspensions was also monitored by *in situ* EPR spectroscopy.

2. Results and Discussion

2.1. Spin Trapping in the Aqueous TiO_2 Suspensions

Despite the fact that the detection of hydroxyl radicals upon UVA irradiation of the aerated aqueous TiO_2 suspensions in the presence of 5,5-dimethyl-1-pyrroline *N*-oxide (DMPO) spin trap represents a frequently applied EPR technique [38–45,49], in order to bring the complete information on the radical species generated in the irradiated TiO_2 in different media we also report the results of EPR spin trapping experiments in aqueous TiO_2 suspensions using different spin trapping agents. As expected, immediately after the irradiation started, a typical four-line EPR signal attributed to $^{\bullet}$DMPO-OH spin-adduct with spin Hamiltonian parameters (a_N = 1.497 mT, a_H = 1.477 mT; g = 2.0057 [50]) was generated in the system TiO_2/DMPO/H_2O/air, as is shown in Figure 2a. The concentration profile of $^{\bullet}$DMPO-OH during the *in situ* EPR spin trapping experiments is strongly influenced by TiO_2 loading, UVA radiation dose, as well as by the initial oxygen and spin trap concentrations [38,44].

Figure 2. The sets of individual EPR spectra (magnetic field sweep width, SW = 8 mT) monitored upon continuous UVA irradiation (λ_{max} = 365 nm; irradiance 15 mW·cm^{-2}) of aerated TiO_2 P25 suspensions in the presence of spin trapping agent DMPO: (**a**) water; (**b**) mixed solvent water/dimethylsulfoxide (5:1 v:v); (**c**) acetonitrile. TiO_2 concentration 0.167 mg·mL^{-1}, $c_{0,DMPO}$ = 0.035 M.

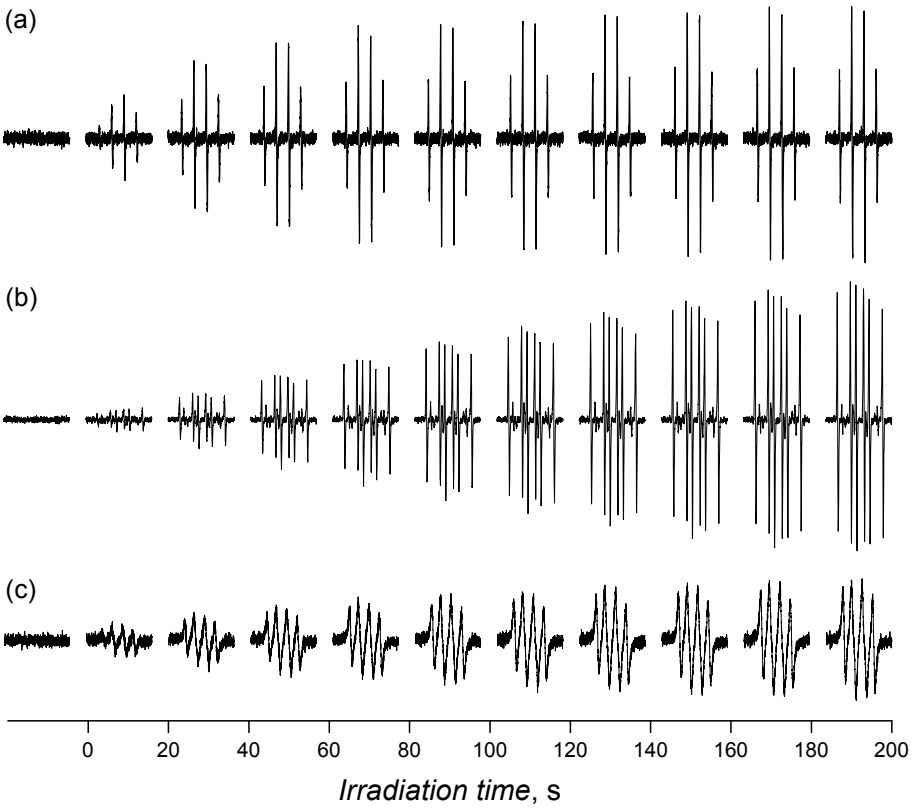

The primary source of the $^{\bullet}$OH radicals in the irradiated aqueous TiO_2 suspensions is the oxidation of OH^- and H_2O by the photogenerated holes, however further reactions of the reactive oxygen species generated in the system leading to $^{\bullet}$OH cannot be excluded (Equations (1)–(6)). The EPR spin trapping

technique is assumed to detect the photogenerated hydroxyl radicals on the photocatalysts' surfaces, based on the previous comparison with the quantification of •OH via fluorescence detection using the hydroxylation of terephthalic acid, by which the bulk •OH are detected [43].

Figure 3 illustrates experimental and simulated EPR spectra of •DMPO-OH measured in the TiO_2 suspensions prepared either using ordinary water, or water enriched with the magnetically active ^{17}O (13%–17% atom.) nucleus. The EPR spectrum depicted in Figure 3b is fully compatible with the presence of both spin-adducts, *i.e.*, •DMPO-OH and •DMPO-^{17}OH [51], unambiguously identifying the adsorbed and close-to-surface water molecules as the source of hydroxyl radicals. Recently, we conducted EPR spin trapping experiments using aerated aqueous suspensions of $Ti^{17}O_2$ (containing up to 90% atom. ^{17}O) with DMPO, and the EPR spectra of •DMPO-OH corresponded to the interaction of one nitrogen nucleus (a_N = 1.492 mT) and one hydrogen nucleus (a_H = 1.476 mT) with an unpaired electron [52]. No evidence of a hyperfine coupling from ^{17}O was found, consequently the lattice oxygens from TiO_2 were excluded as the source of hydroxyl radicals trapped by DMPO under the given experimental conditions [52].

Figure 3. Experimental (**black**) and simulated (**red**) EPR spectra (*SW* = 8 mT) obtained upon irradiation (λ_{max} = 365 nm; irradiance 15 mW·cm^{-2}; exposure 400 s) of the aerated aqueous TiO_2 P25 suspensions in the presence of spin trapping agent DMPO (TiO_2 concentration 0.167 mg·mL^{-1}, $c_{0,DMPO}$ = 0.035 M): (**a**) ordinary water; (**b**) water enriched with $H_2{}^{17}O$ (13%–17% atom.). Simulation parameters (hfcc in mT): (a) •DMPO–OH (a_N = 1.497, a_H = 1.477; g = 2.0057); (b) linear combination of spin-adducts, *i.e.*, •DMPO–OH (relative concentration in %, 82) and •DMPO-^{17}OH (a_N = 1.494, a_H = 1.480, a_{17O} = 0.467; g = 2.0057; 18).

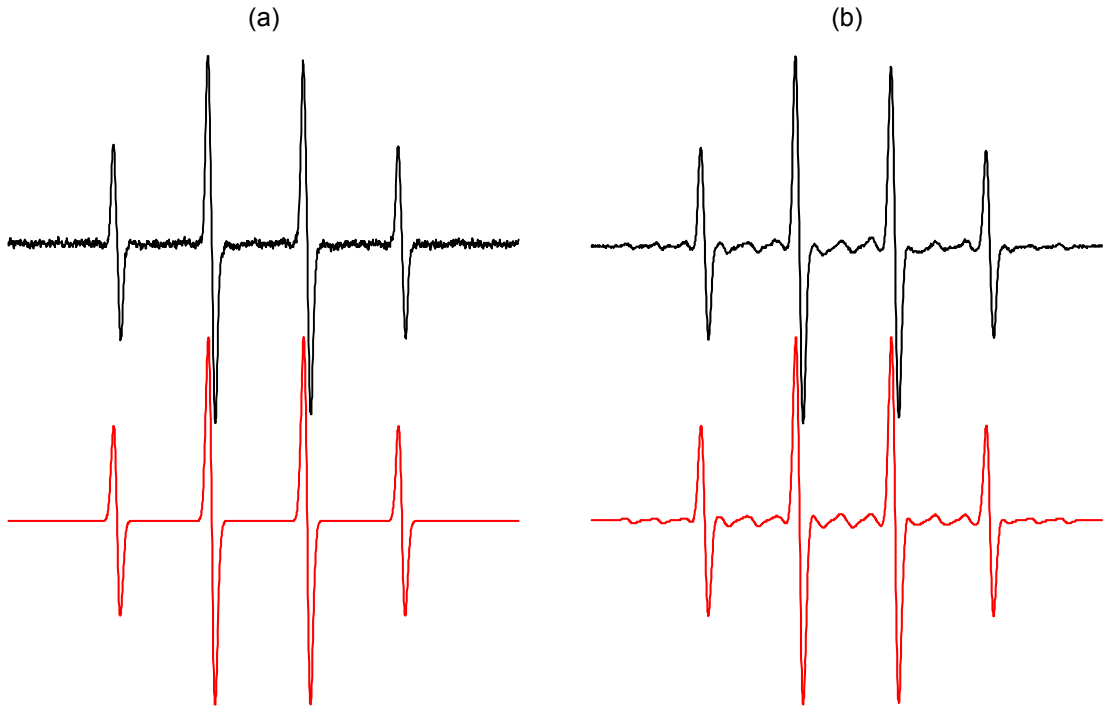

Previously, the possibility of a direct oxidation of the spin trapping agent DMPO via photogenerated holes to a radical cation $DMPO^{\bullet+}$, which subsequently reacts with water molecules forming a so-called imposter spin-adduct $^{\bullet}$DMPO-OH, was supposed [41,43,44]. In addition, the degradation of the low-stability $^{\bullet}$DMPO-O_2H spin-adduct, theoretically also generated in the studied system, results in the $^{\bullet}$DMPO-OH formation [53]. However, the generation of the surface hydroxyl radicals can be evidenced by the addition of dimethylsulfoxide (DMSO) to the aqueous TiO_2 suspensions, since the rapid reaction of hydroxyl radicals with DMSO (Table 1) produces methyl radicals [54], detectable in the reaction with spin trap (ST) as the corresponding carbon-centered spin-adduct, Equations (7) and (8):

$$(CH_3)_2SO + {}^{\bullet}OH \rightarrow CH_3(OH)SO + {}^{\bullet}CH_3 \quad (7)$$

$$ {}^{\bullet}CH_3 + ST \rightarrow {}^{\bullet}ST\text{-}CH_3 \quad (8)$$

Table 1. Bimolecular rate constants for the reaction of hydroxyl radical with the selected solvents [54], decay constants and lifetime of singlet oxygen ($^1\Delta_g$) in selected solvents [55].

Solvent	$k_{\bullet OH}$, $M^{-1}\cdot s^{-1}$	$k_{^1O_2}$, s^{-1}	τ ($1/k_{^1O_2}$), µs
Water	–	2.4×10^5	4.2
Dimethylsulfoxide [#]	7.0×10^9	5.2×10^4	19
Acetonitrile [#]	2.2×10^7	1.4×10^4	71
Methanol [#]	8.3×10^8	1.1×10^5	9
Ethanol [#]	2.2×10^9	7.9×10^4	13

[#]: determined in aqueous solutions.

Figure 2b shows the set of EPR spectra monitored during the exposure of TiO_2/DMPO/air in mixed solvent water/DMSO (5:1 v:v). The EPR spectra obtained are more complex compared to those found in water suspensions (Figure 2a), and represent a superposition of the dominant six-line signal attributed to $^{\bullet}$DMPO-CH_3 and the low-intensity signal of $^{\bullet}$DMPO-OH with slightly modified hyperfine coupling constants (hfcc) caused by the DMSO presence in the system [56]. The experimental and simulated EPR spectra found upon 400 s exposure are depicted in Figure 4a and the corresponding spin Hamiltonian parameters elucidated from the simulated spectra are summarized in Table 2.

Further experiments using 3,5-dibromo-4-nitrosobenzene sulfonate (DBNBS) spin trapping agent in aerated aqueous TiO_2 suspensions containing DMSO or DMSO-d_6 (water/DMSO, 5:1 v:v) unambiguously confirmed the generation of methyl radicals via the reaction of hydroxyl radicals with the solvent, as the EPR spectra monitored upon UVA irradiation are well-matched to $^{\bullet}$DBNBS-CH_3 or $^{\bullet}$DBNBS-CD_3 spin-adducts (Figure 4b,c), respectively, with the spin Hamiltonian parameters well correlated with literature data (Table 2).

Figure 4. Experimental (**black**) and simulated (**red**) EPR spectra obtained upon irradiation (λ_{max} = 365 nm; irradiance 15 mW·cm^{-2}; exposure 400 s) of the aerated TiO_2 P25 suspensions in mixed solvent water/DMSO (5:1 v:v) in the presence of various spin trapping agents (TiO_2 concentration 0.167 mg·mL^{-1}): (**a**) DMPO (*SW* = 8 mT; $c_{0,DMPO}$ = 0.035 M); (**b**) DBNBS (*SW* = 10 mT; $c_{0,DBNBS}$ = 0.008 M); (**c**) DBNBS using DMSO-d_6. The spin Hamiltonian parameters of corresponding spin-adducts are listed in Table 2. (a) •DMPO-CH_3 (relative concentration in %, 94), •DMPO-OH (6); (b) •DBNBS–CH_3 (100); (c) •DBNBS-CD_3 (100).

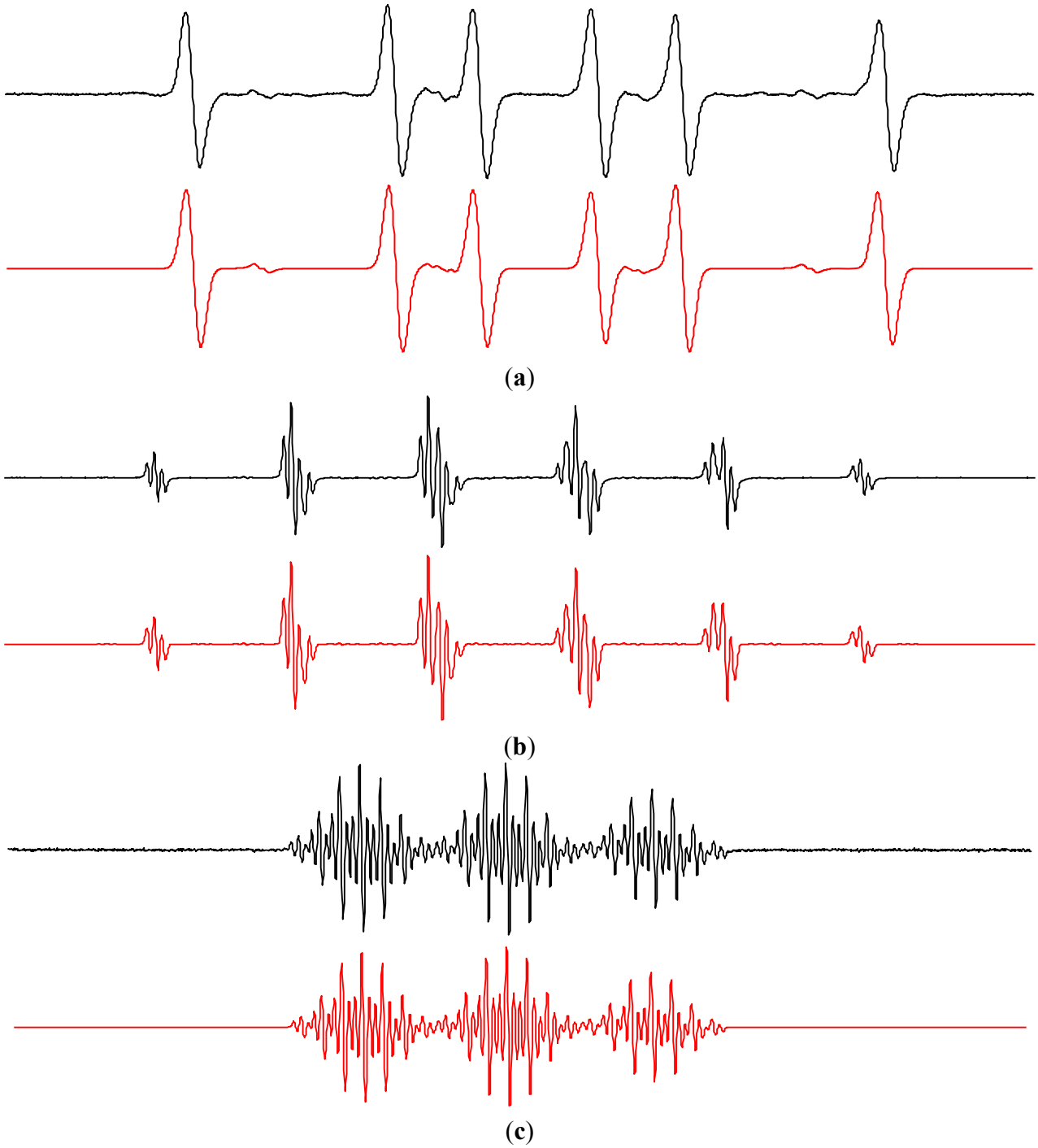

Table 2. Spin Hamiltonian parameters (hyperfine coupling constants and *g*-values) of the spin-adducts elucidated from simulations of the experimental EPR spectra obtained upon UVA irradiation (λ_{max} = 365 nm) of aerated TiO_2 P25 suspensions in water and water/dimethylsulfoxide mixed solvent (5:1 v:v) in the presence of the corresponding spin trapping agents.

Spin-Adduct	Hyperfine Coupling Constants (mT)		*g*-Value	Reference
	a_{NO}	a_i		
Water				
•DMPO–OH	1.497	a_H^{β} = 1.477	2.0057	[50]
•DMPO–^{17}OH	1.494	a_H^{β} = 1.480; a^{17}_O = 0.469	2.0057	[51,57]
•DMPO–N_3	1.481	a_H^{β} = 1.426; a_N = 0.314	2.0057	[50]
***trans*-•EMPO–OH**	1.410	a_H^{β} = 1.278; a_H^{γ} = 0.066; a_H^{γ} = 0.043	2.0056	[58,59]
***cis*-•EMPO–OH**	1.410	a_H^{β} = 1.542	2.0056	[58,59]
•$EMPO_{degr}$	1.514	a_H^{β} = 2.187	2.0056	–
***trans*-•DIPPMPO–OH**	1.410	a_H^{β} = 1.319; a_P = 4.692	2.0055	[59,60]
***cis*-•DIPPMPO–OH**	1.646	a_H^{β} = 1.236; a_P = 3.572	2.0055	[59,60]
•$DIPPMPO_{degr}$	1.469	a_H^{β} = 2.147; a_P = 4.830	2.0055	–
•POBN–OH	1.508	a_H^{β} = 0.169	2.0057	[44]
•$POBN_{degr}$	1.461	a_H^{β} = 1.413	2.0055	[61]
Water/DMSO (5:1 v:v)				
•DMPO–OH	1.469	a_H^{β} = 1.358; a_H^{γ} = 0.067	2.0057	[56]
•DMPO–CH_3	1.588	a_H^{β} = 2.250	2.0055	[50]
•DBNBS–CH_3	1.434	a_H(3H) = 1.331; a_H(2H^m) = 0.069; a^{13}_C = 0.929	2.0063	[50,62]
•DBNBS–CD_3	1.434	a_D(3D) = 0.201; a_H(2H^m) = 0.070	2.0063	[50]

Symbols β and γ denote the position of the interacting hydrogen nuclei.

The application of 5-(ethoxycarbonyl)-5-methyl-1-pyrroline *N*-oxide (EMPO), 5-(diisopropoxyphosphoryl)-5-methyl-1-pyrroline *N*-oxide (DIPPMPO) and α-(4-pyridyl-1-oxide)-*N*-*tert*-butylnitrone (POBN) spin trapping agents suitable for the detection of oxygen-centered radicals in the aerated aqueous TiO_2 suspensions upon exposure confirmed the dominant generation of hydroxyl radical spin-adducts (Figure 5). The chiral centre in EMPO and DIPPMPO molecules may result in the production of *trans* and *cis* spin-adduct diastereoisomers. Indeed, the simulation analysis of the corresponding experimental EPR spectra summarized in Table 2, revealed the superposition of two individual EPR signals belonging to hydroxyl radical spin-adduct diastereoisomers. Additionally, low-intensity EPR signals of radical intermediates originating from the spin traps decomposition were detected as the carbon-centered spinadducts (•$EMPO_{degr}$, •$DIPPMPO_{degr}$) or the four-line signal of hydroxy *tert*-butylnitroxide (•$POBN_{degr}$) [61].

Previously, the photoinduced generation of $O_2^{\bullet-}$ on the irradiated TiO_2 nanoparticles was confirmed by low temperature EPR measurements below 160 K [25,31,32,34,52]. Even though the spin trapping agents EMPO and DIPPMPO were specially designed for the detection of superoxide radical anion in aqueous media and biological systems [60,63–66], the EPR signals reflecting the presence of •EMPO-O_2^-/O_2H and •DIPPMPO-O_2^-/O_2H spin-adducts were not found in the irradiated aqueous TiO_2 suspensions (Figure 5). Most probably, under the given experimental conditions, the superoxide radical anions are preferably transformed to hydrogen peroxide by a disproportionation with protons [24,26,67].

Moreover, a significantly lower rate constants for the addition of $O_2^{\bullet-}$/$^{\bullet}O_2H$ to the nitrone spin traps may cause the limited production of spin-adducts [46,48]. The rapid transformation of superoxide radical anions, as well as their very slow reaction with nitrone spin traps caused that at room temperature in aerated aqueous TiO_2 suspensions superoxide detection using conventional spectroscopic techniques failed, and only chemiluminescence with luminol or luciferin analog was applied as a suitable experimental method [68–70].

Figure 5. Experimental (**black**) and simulated (**red**) EPR spectra obtained upon irradiation (λ_{max} = 365 nm; irradiance 15 mW·cm^{-2}; exposure 400 s) of the aerated aqueous TiO_2 P25 suspensions in the presence of various spin trapping agents (TiO_2 concentration 0.167 mg·mL^{-1}): (**a**) EMPO (*SW* = 8 mT; $c_{0,EMPO}$ = 0.05 M); (**b**) DIPPMPO (*SW* = 16 mT; $c_{0,DIPPMPO}$ = 0.035 M); (**c**) POBN (*SW* = 8 mT; $c_{0,POBN}$ = 0.05 M). Simulations represent linear combinations of corresponding spin-adducts (hfcc parameters listed in Table 2): (a) *trans*-$^{\bullet}$EMPO–OH (relative concentration in %, 68), *cis*-$^{\bullet}$EMPO-OH (28), $^{\bullet}EMPO_{degr}$ (4); (b) *trans*-$^{\bullet}$DIPPMPO-OH (77), *cis*-$^{\bullet}$DIPPMPO-OH (10), $^{\bullet}DIPPMPO_{degr}$ (13); (c) $^{\bullet}$POBN-OH (92), $^{\bullet}POBN_{degr}$ (8).

(**a**)

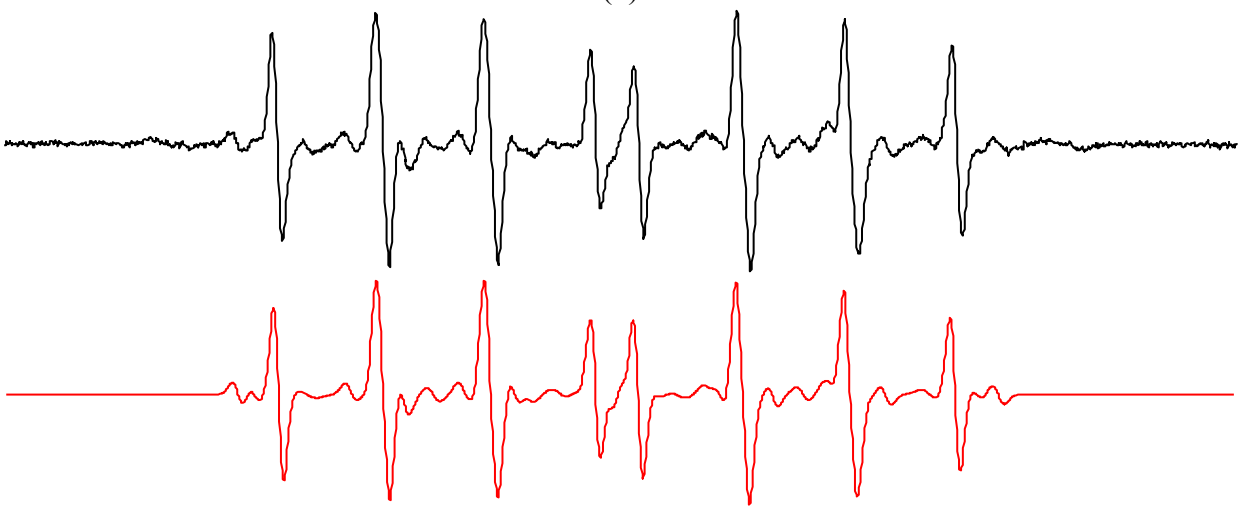

(**b**)

Figure 5. *Cont.*

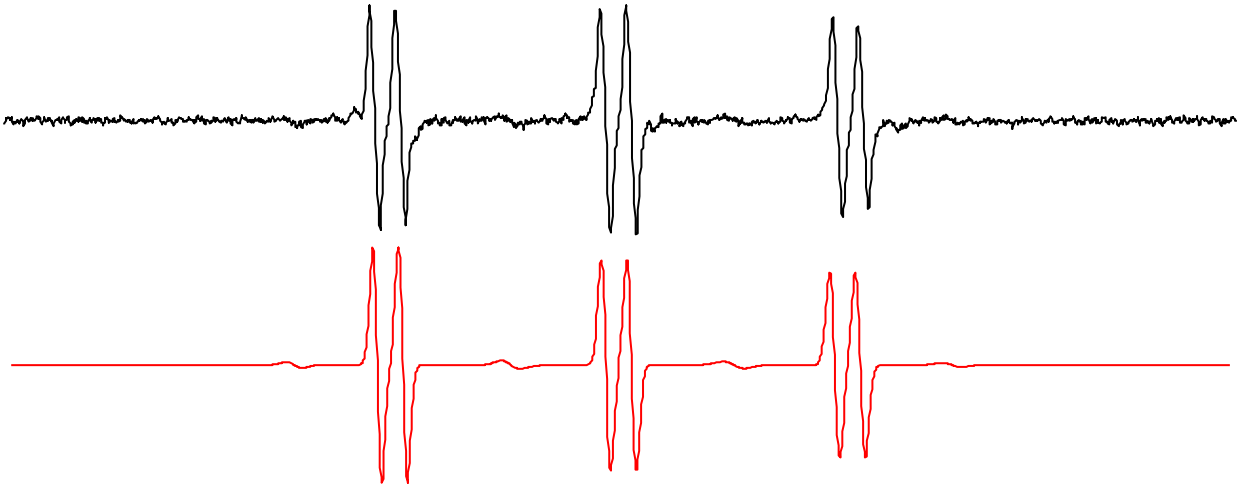

(c)

2.2. Spin Trapping in Non-Aqueous TiO_2 Suspensions

EPR spin trapping investigations of reactive radicals produced in the irradiated TiO_2 dispersions so far were focused mainly on aqueous systems and on the detection of hydroxyl radicals [20,31,35–37,49]. Analogous experiments performed in organic solvents may provide interesting information concerning the radical intermediates generated [13,71–74], consequently we carried out spin trapping experiments with TiO_2 nanoparticles dispersed in DMSO, acetonitrile (ACN), methanol and ethanol. The generation of electron-hole pairs upon TiO_2 irradiation and their consecutive reactions resulting in the free radicals formation are substantially influenced by the solvent properties [54,75,76]. The increased solubility of molecular oxygen plays an important role in these processes (Table 3), together with the stabilization effect of the aprotic solvents on the superoxide radical anions and the reactivity of holes and hydroxyl radicals with the solvents (Table 1).

Table 3. Solubility of molecular oxygen in various solvents at 25 °C.

Solvent	c_{O_2}, mM	Reference
Water	1.0	[77]
Dimethylsulfoxide	2.1	[78]
Acetonitrile	8.1	[78]
Methanol	9.4–10.3	[79]
Ethanol	7.5–11.6	[79]

2.2.1. Dimethylsulfoxide

The EPR spectra monitored upon UVA photoexcitation of TiO_2 suspensions in aerated DMSO (Figure 6a) differ from those found when water was used as a solvent (Figure 3a), and the dominating signals represent spin-adducts $^{\bullet}$DMPO-O_2^- and $^{\bullet}$DMPO-OCH_3 with the spin Hamiltonian parameters summarized in Table 4. The superoxide radical anion stabilization in the aprotic solvent explains its favourable generation and consequently also trapping [24,25]. The production of $^{\bullet}$DMPO-OCH_3 adduct is initiated by the oxidation of hydroxide anions or water molecules adsorbed on the titanium dioxide

surface producing reactive hydroxyl radicals, which immediately attack the DMSO solvent forming methyl radicals (Equation (7)), as shown above in the mixed water/DMSO solvent (Figure 4). The rapid reaction of methyl radicals with molecular oxygen results in the generation of peroxomethyl radicals serving as a source of $^{\bullet}$DMPO–OCH_3 spin-adducts (Equations (9)–(13)) [73]. Further low-intensity oxygen-centered spin-adduct assigned to $^{\bullet}$DMPO–OR originates from the solvent and most probably represents $^{\bullet}$DMPO–$OCH_2S(O)CH_3$:

$$^{\bullet}CH_3 + O_2 \rightarrow CH_3OO^{\bullet} \quad (9)$$

$$DMPO + CH_3OO^{\bullet} \rightarrow {}^{\bullet}DMPO\text{–}OOCH_3 \quad (10)$$

$$2\ {}^{\bullet}DMPO\text{–}OOCH_3 \rightarrow O_2 + 2\ {}^{\bullet}DMPO\text{–}OCH_3 \quad (11)$$

$$2\ CH_3OO^{\bullet} \rightarrow 2\ CH_3O^{\bullet} + O_2 \quad (12)$$

$$DMPO + CH_3O^{\bullet} \rightarrow {}^{\bullet}DMPO\text{–}OCH_3 \quad (13)$$

The photoinduced generation of methyl radicals upon the irradiation of titania-DMSO dispersions was confirmed by the nitroso spin trapping agent DBNBS, suitable for the identification of carbon-centered radicals, as typical signal of $^{\bullet}$DBNBS-CH_3 and $^{\bullet}$DBNBS-CD_3 (using DMSO-d_6) were detected (Figure 6b,c). Depending on the experimental conditions the spin trap decomposition may occur during the photocatalytic processes demonstrated by the generation of $^{\bullet}$DBNBS-SO_3^- (Table 4).

Figure 6. Experimental (**black**) and simulated (**red**) EPR spectra (*SW* = 8 mT) obtained upon irradiation (λ_{max} = 365 nm; irradiance 15 mW·cm^{-2}; exposure 400 s) of the aerated TiO_2 P25 DMSO suspensions in the presence of various spin trapping agents (TiO_2 concentration 0.167 mg·mL^{-1}): (**a**) DMPO ($c_{0,DMPO}$ = 0.035 M); (**b**) DBNBS ($c_{0,DBNBS}$ = 0.008 M); (**c**) DBNBS using DMSO-d_6 (83% vol.). The spin Hamiltonian parameters of corresponding spin-adducts are listed in Table 4. (**a**) $^{\bullet}$DMPO–O_2^- (relative concentration in %, 46), $^{\bullet}$DMPO–OCH_3 (46), $^{\bullet}$DMPO–OR (6), $^{\bullet}$DMPO–CH_3 (2); (**b**) $^{\bullet}$DBNBS–CH_3 (90), $^{\bullet}$DBNBS–SO_3^- (10); (**c**) $^{\bullet}$DBNBS–CD_3 (86), $^{\bullet}$DBNBS–CH_3 (14).

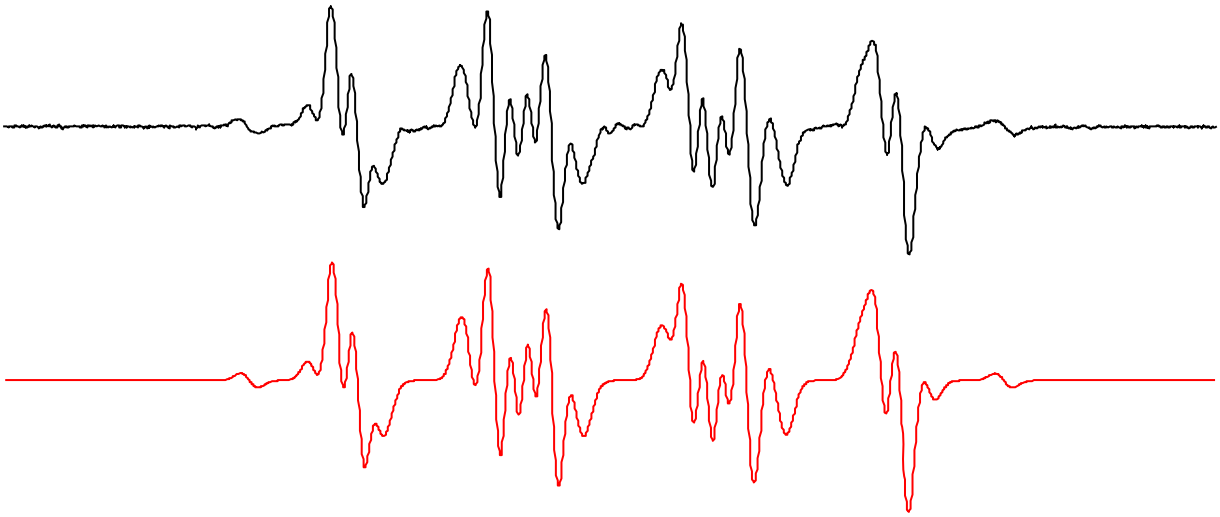

(**a**)

Figure 6. *Cont.*

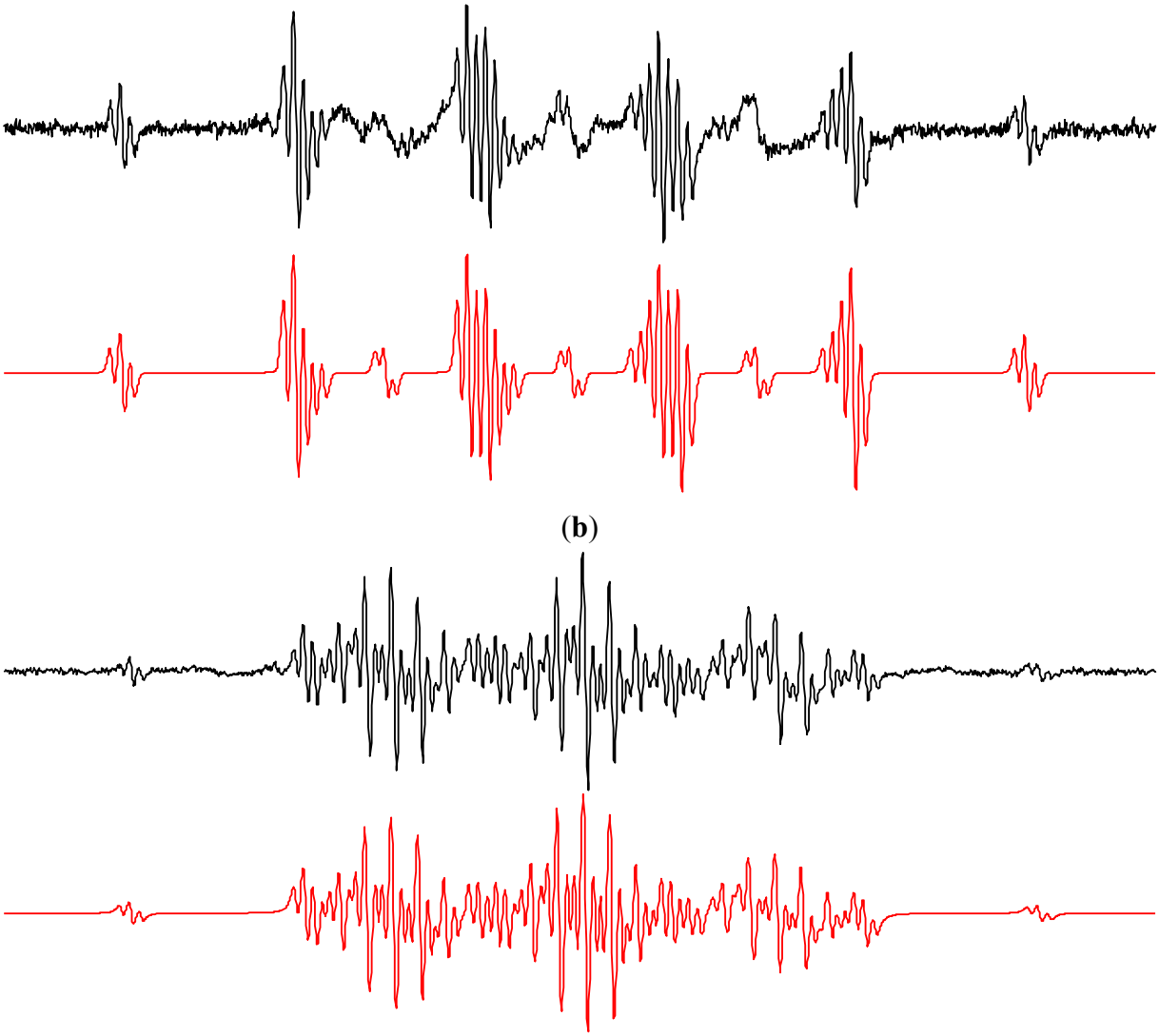

(**b**)

(**c**)

2.2.2. Acetonitrile

Due to the increased solubility of molecular oxygen in ACN (Table 3) the EPR spectra monitored in the irradiated systems TiO_2/DMPO/ACN/air represent a four-line EPR signal with significantly broadened spectral lines (Figure 2c, Figure 7 blue line). Consequently, to obtain spectra suitable for the identification of spin-adduct parameters, the saturation of the exposed sample with argon is necessary. The experimental EPR spectrum recorded immediately after a post-radiation Ar-saturation and EPR spectrometer re-tuning, along with its simulation is shown in Figure 7 (black and red lines). Acetonitrile as an aprotic solvent stabilizes superoxide radical anions, consequently the spin-adduct $^{\bullet}$DMPO-O_2^- dominates the EPR spectrum. The use of dried ACN solvent indicates that the hydroxyl radicals are generated by the oxidation of OH^-/H_2O adsorbed on the TiO_2 surface via the photogenerated holes [80]. A lower reactivity of the photogenerated hydroxyl radicals towards acetonitrile (Table 1) allows the hydroxyl radicals to be trapped by DMPO and the $^{\bullet}$DMPO-OH was found in the spectra (Figure 7). The formation of $^{\bullet}$DMPO-OCH_3 most probably relates to the

interaction of hydroxyl radicals with the solvent [81] producing $CH_3OO^{\bullet}$ radicals trapped as the $^{\bullet}$DMPO-OCH_3 spin-adducts [73]. The spin Hamiltonian parameters of the individual spin-adducts elucidated by the simulation of experimental EPR spectra obtained in TiO_2/DMPO/ACN/air are summarized in Table 4.

Figure 7. Experimental (**blue**) EPR spectra (*SW* = 8 mT) obtained upon irradiation (λ_{max} = 365 nm; irradiance 15 mW·cm^{-2}; exposure 400 s) of the aerated TiO_2 P25 (0.167 mg·mL^{-1}) suspensions in ACN containing DMPO spin trap ($c_{0,DMPO}$ = 0.035 M), along with EPR spectra measured after post-radiation saturation with argon (**black**) and their simulations (**red**). The spin Hamiltonian parameters of corresponding spin-adducts are listed in Table 4. $^{\bullet}$DMPO-O_2^- (rel. conc. in %, 60), $^{\bullet}$DMPO–OH (9), $^{\bullet}$DMPO-OCH_3 (23), $^{\bullet}$$DMPO_{degr}$ (8).

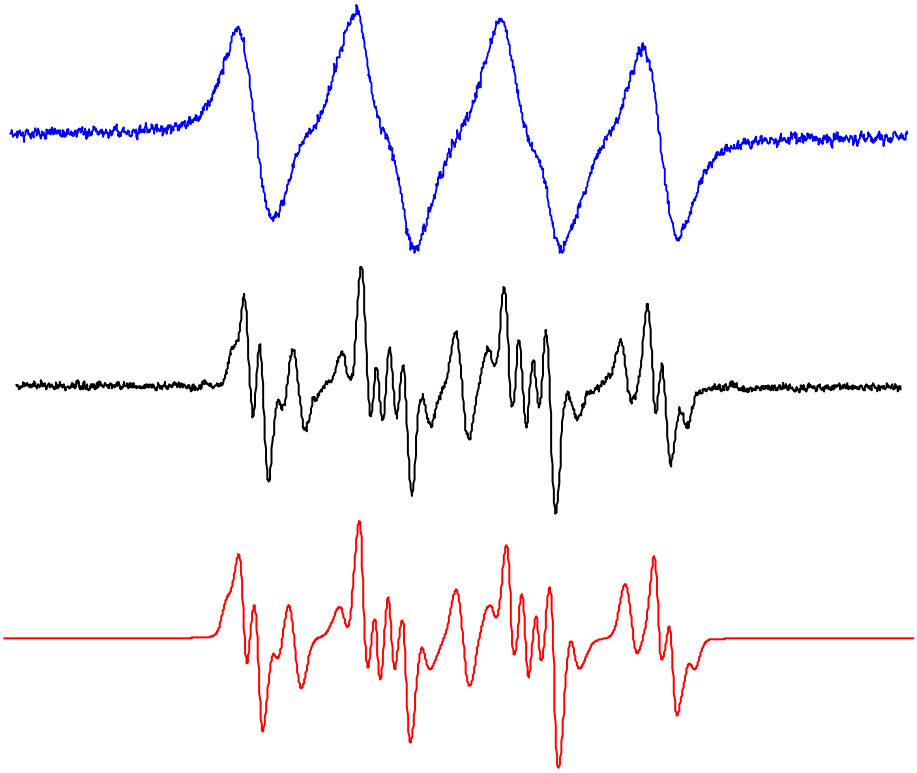

Additional experiments with nitrosodurene (ND) spin trap were performed in order to identify the structure of the carbon-centered radicals produced during the exposure of TiO_2/ACN/air. The EPR spectra measured upon continuous irradiation (spectra not shown) revealed the presence of a nine-line signal of $^{\bullet}$ND–CH_2CN, produced via the interaction of $^{\bullet}$OH with ACN [54], and a broad, three-line signal of $ND^{\bullet+}$ generated by the spin trap oxidation (Table 4).

2.2.3. Methanol and Ethanol

The protic solvents methanol and ethanol are characterized with increased concentration of dissolved molecular oxygen (Table 3), and these solvents are well-known as efficient scavengers of photogenerated holes [82]. By their application radical intermediates created via interaction with both photogenerated charge carriers may be observed, *i.e.*, electrons are scavenged by molecular oxygen

forming $O_2^{\bullet-}$ and holes react with alcohols producing the primary alkoxy radical species, $^{\bullet}OCH_3$ and $^{\bullet}OCH_2CH_3$ (Equations (14) and (15)) [12,13,62].

$$CH_3OH + h^+ \rightarrow CH_3O^{\bullet} + H^+ \quad (14)$$

$$CH_3CH_2OH + h^+ \rightarrow CH_3CH_2O^{\bullet} + H^+ \quad (15)$$

Table 4. Spin Hamiltonian parameters (hyperfine coupling constants and *g*-values) of spin-adducts elucidated from the simulations of experimental EPR spectra obtained upon UVA irradiation (λ_{max} = 365 nm) of aerated TiO_2 P25 suspensions in organic solvents in the presence of spin traps.

Spin-Adduct	Hyperfine Coupling Constants (mT)		*g*-Value	Reference
	a_{NO}	a_i		
DMSO				
$^{\bullet}$DMPO–O_2^-	1.287	a_H^{β} = 1.041; a_H^{γ} = 0.139	2.0057	[25,50,83]
$^{\bullet}$DMPO–OCH_3	1.329	a_H^{β} = 0.808; a_H^{γ} = 0.164	2.0057	[50,84]
$^{\bullet}$DMPO–OR	1.301	a_H^{β} = 1.464	2.0057	[84]
$^{\bullet}$DMPO–CH_3	1.462	a_H^{β} = 2.093	2.0056	[50]
$^{\bullet}$DBNBS–CH_3	1.337	a_H(3H) = 1.211; a_H(2H^m) = 0.067	2.0064	[50]
$^{\bullet}$DBNBS–CD_3	1.334	a_D(3D) = 0.183; a_H(2H^m) = 0.067	2.0064	[50]
$^{\bullet}$DBNBS–SO_3^-	1.295	a_H(2H^m) = 0.054	2.0064	[85]
ACN				
$^{\bullet}$DMPO–O_2^- #	1.296	a_H^{β} = 1.044; a_H^{γ} = 0.133	2.0057	[50,74]
$^{\bullet}$DMPO–OH #	1.382	a_H^{β} = 1.200; a_H^{γ} = 0.080	2.0057	[74]
$^{\bullet}$DMPO–OCH_3 #	1.312	a_H^{β} = 0.796; a_H^{γ} = 0.179	2.0057	[74]
$^{\bullet}$DMPO$_{degr}$ #	1.479		2.0056	–
$^{\bullet}$ND–CH_2CN	1.342	a_H(2H) = 0.977	2.0057	[86,87]
ND$^{\bullet+}$	2.608		2.0057	[50]
Methanol				
$^{\bullet}$DMPO–O_2^- #	1.376	a_H^{β} = 0.963; a_H^{γ} = 0.132	2.0057	[50]
$^{\bullet}$DMPO–OCH_3 #	1.363	a_H^{β} = 0.775; a_H^{γ} = 0.167	2.0057	[50]
$^{\bullet}$DMPO–OCH_2OH #	1.414	a_H^{β} = 1.266; a_H^{γ} = 0.075	2.0057	[50]
$^{\bullet}$DMPO–CH_2OH #	1.506	a_H^{β} = 2.116	2.0056	[50]
$^{\bullet}$DMPO$_{degr}$ #	1.523		2.0056	–
$^{\bullet}$ND–CH_2OH	1.387	a_H(2H) = 0.771	2.0057	[62,86,87]
Ethanol				
$^{\bullet}$DMPO–O_2^- #	1.322	a_H^{β} = 1.050; a_H^{γ} = 0.133	2.0057	[50]
$^{\bullet}$DMPO–OCH_2CH_3 #	1.356	a_H^{β} = 0.761; a_H^{γ} = 0.174	2.0057	[50]
$^{\bullet}$DMPO–OR #	1.470	a_H^{β} = 1.094; a_H^{γ} = 0.090	2.0057	[50]
$^{\bullet}$DMPO–CR_1 #	1.481	a_H^{β} = 2.195	2.0056	[50]
$^{\bullet}$DMPO–CR_2 #	1.534	a_H^{β} = 2.215	2.0056	[50]
$^{\bullet}$ND–$CH(CH_3)OH$	1.398	a_H = 0.702	2.0057	[62,86,87]
$^{\bullet}$ND–CH_3	1.452	a_H(3H) = 1.345	2.0057	[62,86,87]

#: post-radiation saturation with argon. Symbols β and γ denote the position of the interacting hydrogen nuclei.

These oxygen-centered radical species can be easily identified using the DMPO spin trap. Due to the higher concentration of dissolved oxygen in these solvents, the EPR spectra of spin-adducts

measured in aerated methanol and ethanol TiO_2 suspensions are characterized by a significant line broadening, which hinders a detailed simulation analysis (Figure 8a,b blue lines). However, the post-radiation saturation of the TiO_2 suspensions with argon, and subsequent measurement of EPR spectra provide the EPR signals of sufficient quality (Figure 8a,b black lines).

Figure 8. Experimental (**blue**) EPR spectra (*SW* = 8 mT) obtained upon irradiation (λ_{max} = 365 nm; irradiance 15 mW·cm^{-2}; exposure 400 s) of the aerated TiO_2 P25 (0.167 mg·mL^{-1}) suspensions in organic solvents containing DMPO spin trap ($c_{0,DMPO}$ = 0.035 M), along with EPR spectra measured after post-radiation saturation with argon (**black**) and their simulations (**red**): (**a**) methanol; (**b**) ethanol. The spin Hamiltonian parameters of corresponding spin-adducts are listed in Table 4. (a) •DMPO–O_2^- (rel. conc. in %, 33), •DMPO–OCH_3 (35), •DMPO–OCH_2OH (21), •DMPO–CH_2OH (7), •$DMPO_{degr}$ (4); (b) •DMPO–O_2^- (17), •DMPO–OCH_2CH_3 (59), •DMPO–OR (10), •DMPO–CR_1 (9), •DMPO–CR_2 (5).

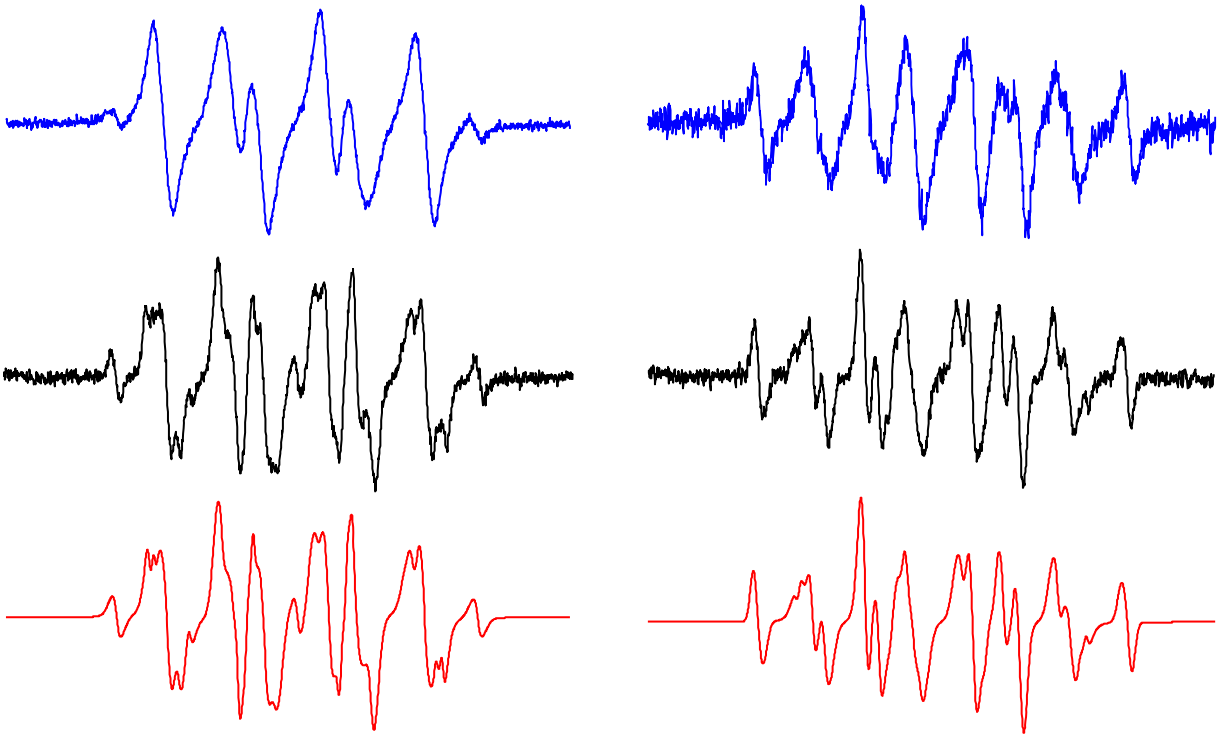

(**a**) (**b**)

Simulations of the EPR spectra measured using this experimental procedure in the system TiO_2/DMPO/methanol revealed the presence of individual DMPO spin-adducts corresponding to •DMPO-O_2^-, •DMPO-OCH_3, •DMPO-CH_2OH, •DMPO-OCH_2OH and a triplet signal assigned to the DMPO degradation product (Figure 8a red line). The spin Hamiltonian parameters of the identified spin-adducts are gathered in Table 4. We assume that the radical species •CH_2OH and •OCH_2OH are produced via complex reactions of •OCH_3 radicals with methanol molecules and molecular oxygen [62], an alternative mechanism of •CH_2OH generation represents the hydrogen abstraction from methanol via hydroxyl radicals (Table 1, Equations (16) and (17)).

$$CH_3O^{\bullet} + CH_3OH \rightarrow CH_3OH + {}^{\bullet}CH_2OH \quad (16)$$

$$CH_3OH + {}^{\bullet}OH \rightarrow {}^{\bullet}CH_2OH + H_2O \quad (17)$$

Simulation of the EPR spectra obtained in the irradiated suspensions TiO_2/DMPO/ethanol after the saturation with argon evidenced the presence of spin-adducts characteristic for $^{\bullet}$DMPO-O_2^-, $^{\bullet}$DMPO-OCH_2CH_3, $^{\bullet}$DMPO-OR, and two carbon-centered spin-adducts with slightly differing hyperfine coupling constants (Figure 8b, Table 4). Nitrosodurene spin trapping agent was used in the analogous experiments to identify the carbon-centered radicals in the irradiated methanol or ethanol TiO_2 suspensions (spectra not shown). In methanol only the generation of $^{\bullet}$ND-CH_2OH was evidenced. The EPR spectra monitored in TiO_2/ethanol suspensions are compatible with $^{\bullet}$ND-$CH(OH)CH_3$ and $^{\bullet}$ND-CH_3 spin-adducts in good accordance with the reactions of ethoxy, 1-hydroxyethyl and 2-hydroxyethyl radicals in ethanol (Equations (18)–(20)) published previously [62], and also with two DMPO carbon-centered spin-adducts detected:

$$CH_3CH_2O^{\bullet} + CH_3CH_2OH \rightarrow CH_3CH_2OH + CH_3{}^{\bullet}CHOH \quad (18)$$

$$CH_3{}^{\bullet}CHOH + CH_3CH_2OH \rightarrow {}^{\bullet}CH_2CH_2OH + CH_3CH_2OH \quad (19)$$

$$CH_2{}^{\bullet}CH_2OH \rightarrow {}^{\bullet}CH_3 + CH_2O \quad (20)$$

2.3. Oxidation of Sterically Hindered Amine in TiO_2 Suspensions

The irradiation of titanium dioxide nanoparticles in the presence of molecular oxygen results in the generation of singlet oxygen, but the specific mechanism of $^1O_2$ formation is not straightforward and alternative reaction pathways have been suggested [88–90]. The direct detection of $^1O_2$ is based on the phosphorescence measurement at 1270 nm corresponding to the radiative transition $O_2(^1\Delta_g) \rightarrow O_2(^3\Sigma_g)$ [89,91]. The principle of the indirect techniques of $^1O_2$ monitoring is the specific reaction with an organic compound generating a product detectable by a suitable method [92], supported by the application of $^1O_2$ scavengers and traps, or using the effect of deuterated solvents. The photoinduced formation of singlet oxygen in the homogeneous systems is frequently monitored also by EPR spectroscopy, detecting the generation of nitroxide radicals derived from 4(R)-2,2,6,6-tetramethylpiperide *N*-oxyl (R = hydroxy, oxo) produced by the oxidation of corresponding sterically hindered amines (SHA) [84,93,94]. Although this method is widely used for the singlet oxygen detection, many questions arise concerning its selectivity [95]. Particular problems may appear when a numerous ROS or other reactive species are formed in the studied system and their interaction with SHA cannot be excluded, e.g., in the irradiated TiO_2 suspensions. The detailed analysis of paramagnetic species generated in homogeneous ACN solutions and TiO_2 suspensions in the presence SHA and ROS was performed previously in our laboratory [74].

The concentration of molecular oxygen in aqueous TiO_2 suspensions play an important role during the oxidation of 4-oxo-2,2,6,6-tetramethylpiperidine (TMPO) to the radical product 2,2,6,6-tetramethylpiperidine *N*-oxyl (Tempone; a_N = 1.617 mT, $a_{^{13}C}(4^{13}C)$ = 0.610 mT; g = 2.0054). In the photoexcited system TiO_2/TMPO/water/air the concentrations of Tempone was very low, and the prolonged irradiation led to a total disappearance of the EPR signal (data not shown). However, the saturation of the aqueous TiO_2 suspension by oxygen led to the continuous growth of the EPR signal of Tempone (a_N = 1.479 mT; g = 2.0057) as shown in Figure 9a. The addition of sodium azide, a widely used water-soluble singlet oxygen quencher, to the TiO_2/TMPO/water/O_2 systems completely

suppressed the Tempone generation. However this result should be very carefully analyzed, since besides the singlet oxygen, azide anions also react very fast with the hydroxyl radicals ($k = 1.4 \times 10^{10}$ M^{-1} s^{-1} [55]) producing the azide radical $^{\bullet}N_3$ [96] detected here as the corresponding spin-adduct $^{\bullet}$DMPO-N_3 in the photoexcited system TiO_2/DMPO/water/NaN_3/air (Table 2). Despite the limited water solubility of β-carotene, an analogous inhibition of TMPO photooxidation was observed also when β-carotene as an effective singlet oxygen quencher [97] was added to the TiO_2 suspensions (Figure 9b). However, due to the lack of specificity the alternative reaction pathways of β-carotene with the radical species generated in the irradiated titania suspensions must be considered [98]. The role of hydroxyl radicals in the SHA oxidation was further demonstrated in the mixed solvent containing DMSO, where the total inhibition of Tempone formation was found, due to the effective scavenging of hydroxyl radicals by DMSO (Figure 9c). The increased concentration of dissolved molecular oxygen in acetonitrile (Table 3), as well as longer lifetime of $^1O_2$ in this solvent (Table 1) resulted in the effective oxidation of TMPO to Tempone. The higher $^3O_2$ concentration in the systems TiO_2/TMPO/ACN/air is reflected also in the spectral linewidth growth with not-resolved ^{13}C-satellites (Figure 9d).

Figure 9. The sets of individual EPR spectra (*SW* = 8 mT) monitored upon continuous UVA irradiation (λ_{max} = 365 nm; irradiance 15 mW·cm^{-2}) of aerated TiO_2 P25 suspensions in the presence of sterically hindered amine TMPO: (**a**) oxygenated water; (**b**) oxygenated water saturated with β-carotene; (**c**) oxygenated mixed solvent water/DMSO (5:1 v:v); (**d**) aerated ACN. TiO_2 concentration 0.167 mg·mL^{-1}, $c_{0,TMPO}$ = 0.008 M.

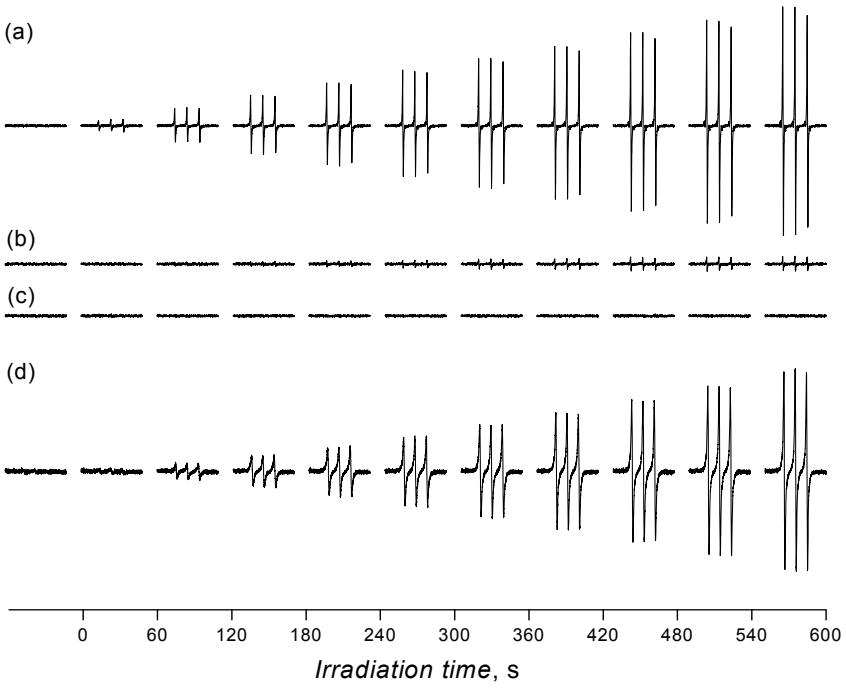

3. Experimental Section

The commercial titanium dioxide Aeroxide® P25 (Evonic Degussa, Essen, Germany) was used and stock suspensions containing 1 mg TiO_2 mL^{-1} were prepared in redistilled water, dimethylsulfoxide (Merck, Darmstadt, Germany, SeccoSolv®, max. 0.025% H_2O), acetonitrile (Merck, SeccoSolv®,

max. 0.005% H_2O), methanol (spectroscopic grade, Lachema, Brno, Czech Republic), and ethanol (for UV spectroscopy, MikroChem, Pezinok, Slovak Republic). The isotopically enriched water-^{17}O (20%–24.9% atom. ^{17}O) and deuterated DMSO-d_6, both from Sigma-Aldrich (Buchs, Switzerland), were used as co-solvents. The stock TiO_2 suspensions were homogenized for 1 min using ultrasound (Ultrasonic Compact Cleaner TESON 1; Tesla, Piešťany, Slovak Republic). The spin trapping agent 5,5-dimethyl-1-pyrroline *N*-oxide (DMPO, Sigma-Aldrich) was distilled prior to use. 5-(Diisopropoxyphosphoryl)-5-methyl-1-pyrroline *N*-oxide (DIPPMPO, Enzo Life Sciences, Farmingdale, NY, USA), 5-(ethoxycarbonyl)-5-methyl-1-pyrroline *N*-oxide (EMPO; Enzo Life Sciences), α-(4-pyridyl-1-oxide)-*N*-*tert*-butylnitrone (POBN; Janssen Chimica, Geel, Belgium), 2,3,5,6,-tetramethylnitrosobenzene (nitrosodurene, ND, Sigma-Aldrich) and 3,5-dibromo-4-nitrosobenzene sulfonate (DBNBS, Sigma-Aldrich) were used without extra purification. All spin traps were stored at −18 °C. The stock solutions of the spin trapping agents were prepared in studied solvents, apart from the ND, characteristic with a limited solubility in polar solvents, which was applied in a saturated suspension directly before the specific experiments. The concentrations of spin traps applied were chosen in order to minimize the undesired photochemical reactions of the spin traps and to gain the effective trapping of photogenerated radical species. The sterically hindered amine 4-oxo-2,2,6,6-tetramethylpiperidine (TMPO, Merck-Schuchardt, Hohenbrunn, Germany) was used as supplied. Sodium azide (analytical grade, Sigma-Aldrich) and β-carotene (UV grade, Sigma-Aldrich) were applied as the singlet oxygen quenchers. Concentrations of the photogenerated paramagnetic species were determined using solutions of 4-oxo-2,2,6,6-tetramethylpiperidine *N*-oxyl (Tempone, Sigma-Aldrich) as the calibration standards.

The TiO_2 P25 suspensions containing the spin trapping agent or the TMPO was mixed and carefully saturated with air or oxygen using a slight gas stream immediately before the EPR measurement. So prepared samples were transferred to a small quartz flat cell (WG 808-Q, optical cell length 0.04 cm; Wilmad-LabGlass, Vineland, NJ, USA) optimized for the TE_{102} cavity (Bruker, Rheinstetten, Germany) of the spectrometer X-band EPR spectrometer (EMXplus, Bruker). During the EPR photochemical experiments the samples were irradiated at 295 K directly in the EPR resonator, and the EPR spectra were recorded *in situ* during a continuous photoexcitation or after a defined exposure. As an irradiation source a UV LED monochromatic radiator (λ_{max} = 365 nm; Bluepoint LED, Hönle UV Technology, Gräfelfing/München, Germany) was used. The irradiance value (λ_{max} = 365 nm; 15 $mW \cdot cm^{-2}$) within the EPR cavity was determined using a UVX radiometer (UVP, Upland, CA, USA). In some cases, argon saturation needed to be applied after the irradiation of the aerated suspensions prior to the subsequent EPR experiment to get better resolved spectra by suppressing the line-broadening effect of molecular oxygen.

Typical EPR spectrometer settings in a standard photochemical experiment were: microwave frequency, ~9.424 GHz; microwave power, 10.53 mW; center field, 335.6 mT; sweep width, 8–16 mT; gain, 1×10^5 to 1×10^6; modulation amplitude, 0.05–0.1 mT; scan, 20 s; time constant, 10.24 ms. The *g*-values (±0.0001) were determined using a built-in magnetometer. The EPR spectra so obtained were analyzed and simulated using the Bruker software WinEPR and SimFonia and the Winsim2002 [99].

4. Conclusions

The EPR spin trapping experiments using a variety of spin trapping agents (DMPO, EMPO, DIPPMPO, POBN, DBNBS and ND) were performed to identify reactive intermediates formed upon irradiation of TiO_2 suspended in water and organic solvents. The role of water in the photoinduced generation of the hydroxyl radical spin-adduct •DMPO-OH in aerated aqueous TiO_2 systems was evidenced using ^{17}O-enriched water. Application of a water-soluble nitroso spin trapping agent DBNBS confirmed the production of methyl radicals when DMSO was added to the aqueous TiO_2 suspensions and the addition of DMSO-d_6 revealed also the origin of these radicals. The photoexcitation of TiO_2 in non-aqueous solvents (DMSO, ACN, methanol and ethanol) in the presence of spin trapping agents showed the stabilization of superoxide radical anions generated via electron transfer reaction to molecular oxygen, as well as the production of various oxygen- and carbon-centered radicals from the solvents. The oxidation of sterically hindered amine TMPO to radical Tempone via ROS was monitored in aqueous and acetonitrile TiO_2 suspensions.

The results obtained demonstrate that indirect EPR spectroscopy techniques represent valuable tools for the characterization of radical intermediates generated in irradiated TiO_2 suspensions. However, a careful selection of the experimental conditions and a precise analysis of the experimental EPR spectra considering alternative reaction pathways is an important aspect of any successful application of these indirect techniques in the characterization of TiO_2 photoactivity.

Supplementary Materials

Supplementary materials can be accessed at: http://www.mdpi.com/1420-3049/19/11/17279/s1.

Acknowledgments

This work was financially supported by Scientific Grant Agency of the Slovak Republic (Project VEGA 1/0289/12) and Slovak University of Technology in Bratislava Young Researcher Grant (Z. Barbieriková).

Author Contributions

Dana Dvoranová and Vlasta Brezová designed experimental research; Dana Dvoranová, Zuzana Barbieriková and Vlasta Brezová performed analysis of experimental data and wrote the paper. All authors read and approved the final manuscript.

Conflicts of Interest

The authors declare no conflict of interest.

References

1. Minero, C.; Maurino, V.; Vione, D. Photocatalytic mechanisms and reaction pathways drawn from kinetic and probe molecules. In *Photocatalysis and Water Purification: From Fundamentals to Recent Applications*, 1st ed.; Pichat, P., Ed.; Wiley-VCH: Weinheim, Germany, 2013; pp. 53–72.

2. Fujishima, A.; Zhang, X.; Tryk, D. TiO_2 photocatalysis and related surface phenomena. *Surf. Sci. Rep.* **2008**, *63*, 515–582.
3. McCullagh, C.; Robertson, J.; Bahnemann, D.; Robertson, P. The application of TiO_2 photocatalysis for disinfection of water contaminated with pathogenic micro-organisms: A review. *Res. Chem. Intermed.* **2007**, *33*, 359–375.
4. Agrios, A.; Pichat, P. State of the art and perspectives on materials and applications of photocatalysis over TiO_2. *J. Appl. Electrochem.* **2005**, *35*, 655–663.
5. Carp, O.; Huisman, C.; Reller, A. Photoinduced reactivity of titanium dioxide. *Prog. Solid State Chem.* **2004**, *32*, 33–177.
6. Shi, H.; Magaye, R.; Castranova, V.; Zhao, J. Titanium dioxide nanoparticles: A review of current toxicological data. *Part. Fibre Toxicol.* **2013**, *10*, 15.
7. Kanakaraju, D.; Glass, B.; Oelgemoller, M. Titanium dioxide photocatalysis for pharmaceutical wastewater treatment. *Environ. Chem. Lett.* **2014**, *12*, 27–47.
8. Lang, X.; Ma, W.; Chen, C.; Ji, H.; Zhao, J. Selective aerobic oxidation mediated by TiO_2 photocatalysis. *Acc. Chem. Res.* **2014**, *47*, 355–363.
9. Ahmed, S.; Rasul, M.; Martens, W.; Brown, R.; Hashib, M. Advances in heterogeneous photocatalytic degradation of phenols and dyes in wastewater: A review. *Water Air Soil Pollut.* **2011**, *215*, 3–29.
10. Gaya, U.; Abdullah, A. Heterogeneous photocatalytic degradation of organic contaminants over titanium dioxide: A review of fundamentals, progress and problems. *J. Photochem. Photobiol. C Rev.* **2008**, *9*, 1–12.
11. McCullagh, C.; Skillen, N.; Adams, M.; Robertson, P. Photocatalytic reactors for environmental remediation: A review. *J. Chem. Technol. Biotechnol.* **2011**, *86*, 1002–1017.
12. Amadelli, R.; Samiolo, L.; Maldotti, A.; Molinari, A.; Gazzoli, D. Selective photooxidation and photoreduction processes at TiO_2 surface-modified by grafted vanadyl. *Int. J. Photoenergy* **2011**, *2011*, doi:10.1155/2011/259453.
13. Molinari, A.; Montoncello, M.; Rezala, H.; Maldotti, A. Partial oxidation of allylic and primary alcohols with O_2 by photoexcited TiO_2. *Photochem. Photobiol. Sci.* **2009**, *8*, 613–619.
14. Henderson, M. A surface science perspective on TiO_2 photocatalysis. *Surf. Sci. Rep.* **2011**, *66*, 185–297.
15. Diebold, U. Structure and properties of TiO_2 surfaces: A brief review. *Appl. Phys. A: Mater. Sci. Process.* **2003**, *76*, 681–687.
16. Pelaez, M.; Nolan, N.; Pillai, S.; Seery, M.; Falaras, P.; Kontos, A.; Dunlop, P.; Hamilton, J.; Byrne, J.; O'Shea, K.; *et al*. A review on the visible light active titanium dioxide photocatalysts for environmental applications. *Appl. Catal. B* **2012**, *125*, 331–349.
17. Diebold, U. The surface science of titanium dioxide. *Surf. Sci. Rep.* **2003**, *48*, 53–229.
18. Zhang, J.; Nosaka, Y. Mechanism of the OH radical generation in photocatalysis with TiO_2 of different crystalline types. *J. Phys. Chem. C* **2014**, *118*, 10824–10832.
19. Montoya, J.; Ivanova, I.; Dillert, R.; Bahnemann, D.; Salvador, P.; Peral, J. Catalytic role of surface oxygens in TiO_2 photooxidation reactions: Aqueous benzene photooxidation with $Ti^{18}O_2$ under anaerobic conditions. *J. Phys. Chem. Lett.* **2013**, *4*, 1415–1422.

20. Salvador, P. On the nature of photogenerated radical species active in the oxidative degradation of dissolved pollutants with TiO_2 aqueous suspensions: A revision in the light of the electronic structure of adsorbed water. *J. Phys. Chem. C* **2007**, *111*, 17038–17043.
21. Green, J.; Carter, E.; Murphy, D. An EPR investigation of acetonitrile reactivity with superoxide radicals on polycrystalline TiO_2. *Res. Chem. Intermed.* **2009**, *35*, 145–154.
22. Carter, E.; Carley, A.; Murphy, D. Evidence for O_2^- radical stabilization at surface oxygen vacancies on polycrystalline TiO_2. *J. Phys. Chem. C* **2007**, *111*, 10630–10638.
23. Berger, T.; Sterrer, M.; Diwald, O.; Knozinger, E.; Panayotov, D.; Thompson, T.; Yates, J. Light-induced charge separation in anatase TiO_2 particles. *J. Phys. Chem. B* **2005**, *109*, 6061–6068.
24. Sawyer, D.T.; Valentine, J.S. How super is superoxide? *Acc. Chem. Res.* **1981**, *14*, 393–400.
25. Harbour, J.R.; Hair, M.L. Detection of superoxide ions in nonaqueous media. Generation by photolysis of pigment dispersions. *J. Phys. Chem.* **1978**, *82*, 1397–1399.
26. Nosaka, Y.; Nosaka, A.Y. Identification and roles of the active species generated on various photocatalysts. In *Photocatalysis and Water Purification: From Fundamentals to Recent Applications*, 1st ed.; Pichat, P., Ed.; Wiley-VCH: Weinheim, Germany, 2013; pp. 3–24.
27. Hirakawa, T.; Yawata, K.; Nosaka, Y. Photocatalytic reactivity for $O_2^{\bullet-}$ and $^{\bullet}OH$ radical formation in anatase and rutile TiO_2 suspension as the effect of H_2O_2 addition. *Appl. Catal. A* **2007**, *325*, 105–111.
28. Hirakawa, T.; Daimon, T.; Kitazawa, M.; Ohguri, N.; Koga, C.; Negishi, N.; Matsuzawa, S.; Nosaka, Y. An approach to estimating photocatalytic activity of TiO_2 suspension by monitoring dissolved oxygen and superoxide ion on decomposing organic compounds. *J. Photochem. Photobiol. A Chem.* **2007**, *190*, 58–68.
29. Wang, Z.; Ma, W.; Chen, C.; Ji, H.; Zhao, J. Probing paramagnetic species in titania-based heterogeneous photocatalysis by electron spin resonance (ESR) spectroscopy—A mini review. *Chem. Eng. J.* **2011**, *170*, 353–362.
30. Micic, O.; Zhang, Y.; Cromack, K.; Trifunac, A.; Thurnauer, M. Trapped holes on TiO_2 colloids studied by electron-paramagnetic-resonance. *J. Phys. Chem.* **1993**, *97*, 7277–7283.
31. Nakaoka, Y.; Nosaka, Y. ESR investigation into the effects of heat treatment and crystal structure on radicals produced over irradiated TiO_2 powder. *J. Photochem. Photobiol. A Chem.* **1997**, *110*, 299–305.
32. Coronado, J.; Maira, A.; Conesa, J.; Yeung, K.; Augugliaro, V.; Soria, J. EPR study of the surface characteristics of nanostructured TiO_2 under UV irradiation. *Langmuir* **2001**, *17*, 5368–5374.
33. Dimitrijevic, N.; Saponjic, Z.; Rabatic, B.; Poluektov, O.; Rajh, T. Effect of size and shape of nanocrystalline TiO_2 on photogenerated charges. An EPR study. *J. Phys. Chem. C* **2007**, *111*, 14597–14601.
34. Kokorin, A.I. Electron Spin Resonance of nanostructured oxide semiconductors. In *Chemical Physics of Nanostructured Semiconductors*; Kokorin, A.I., Bahnemann, D.W., Eds.; VSP BV: Utrecht, The Netherlands, 2003; pp. 203–263.
35. Ghiazza, M.; Alloa, E.; Oliaro-Bosso, S.; Viola, F.; Livraghi, S.; Rembges, D.; Capomaccio, R.; Rossi, F.; Ponti, J.; Fenoglio, I. Inhibition of the ROS-mediated cytotoxicity and genotoxicity of nano-TiO_2 toward human keratinocyte cells by iron doping. *J. Nanopart. Res.* **2014**, *16*, 2263.

36. Chiesa, M.; Paganini, M.C.; Livraghi, S.; Giamello, E. Charge trapping in TiO_2 polymorphs as seen by electron paramagnetic resonance spectroscopy. *Phys. Chem. Chem. Phys.* **2013**, *15*, 9435–9447.
37. Li, M.; Yin, J.J.; Wamer, W.G.; Lo, Y.M. Mechanistic characterization of titanium dioxide nanoparticle-induced toxicity using electron spin resonance. *J. Food Drug Anal.* **2014**, *22*, 76–86.
38. Grela, M.A.; Coronel, M.E.J.; Colussi, A.J. Quantitative spin-trapping studies of weakly illuminated titanium dioxide sols. Implications for the mechanism of photocatalysis. *J. Phys. Chem.* **1996**, *100*, 16940–16946.
39. Jaeger, C.D.; Bard, A.J. Spin trapping and electron spin resonance detection of radical intermediates in the photodecomposition of water at TiO_2 particulate systems. *J. Phys. Chem.* **1979**, *83*, 3146–3152.
40. Dvoranová, D.; Brezová, V.; Mazúr, M.; Malati, M.A. Investigations of metal-doped titanium dioxide photocatalysts. *Appl. Catal. B* **2002**, *37*, 91–105.
41. Taborda, A.V.; Brusa, M.A.; Grela, M.A. Photocatalytic degradation of phthalic acid on TiO_2 nanoparticles. *Appl. Catal. A* **2001**, *208*, 419–426.
42. Brezová, V.; Staško, A.; Biskupič, S.; Blažková, A.; Havlínová, B. Kinetics of hydroxyl radical spin trapping in photoactivated homogeneous (H_2O_2) and heterogeneous (TiO_2, O_2) aqueous systems. *J. Phys. Chem.* **1994**, *98*, 8977–8984.
43. Nosaka, Y.; Komori, S.; Yawata, K.; Hirakawa, T.; Nosaka, A. Photocatalytic $^{\bullet}OH$ radical formation in TiO_2 aqueous suspension studied by several detection methods. *Phys. Chem. Chem. Phys.* **2003**, *5*, 4731–4735.
44. Brezová, V.; Dvoranová, D.; Staško, A. Characterization of titanium dioxide photoactivity following the formation of radicals by EPR spectroscopy. *Res. Chem. Intermed.* **2007**, *33*, 251–268.
45. Brezová, V.; Billik, P.; Vrecková, Z.; Plesch, G. Photoinduced formation of reactive oxygen species in suspensions of titania mechanochemically synthesized from $TiCl_4$. *J. Mol. Catal. A Chem.* **2010**, *327*, 101–109.
46. Hawkins, C.L.; Davies, M.J. Detection and characterisation of radicals in biological materials using EPR methodology. *Biochim. Biophys. Acta Gen. Subj.* **2014**, *1840*, 708–721.
47. Spasojevic, I. Free radicals and antioxidants at a glance using EPR spectroscopy. *Crit. Rev. Clin. Lab. Sci.* **2011**, *48*, 114–142.
48. Alberti, A.; Macciantelli, D. Spin Trapping. In *Electron Paramagnetic Resonance: A Practitioner's Toolkit*; Brustolon, M., Giamelo, E., Eds.; John Wiley & Sons: Hoboken, NJ, USA, 2009; pp. 287–323.
49. Dodd, N.J.F.; Jha, A.N. Photoexcitation of aqueous suspensions of titanium dioxide nanoparticles: An electron spin resonance spin trapping study of potentially oxidative reactions. *Photochem. Photobiol.* **2011**, *87*, 632–640.
50. Buettner, G.R. Spin trapping: ESR parameters of spin adducts. *Free Radic. Biol. Med.* **1987**, *3*, 259–303.
51. Lloyd, R.V.; Hanna, P.M.; Mason, R.P. The origin of the hydroxyl radical oxygen in the Fenton reaction. *Free Radic. Biol. Med.* **1997**, *22*, 885–888.
52. Brezová, V.; Barbieriková, Z.; Zukalová, M.; Dvoranová, D.; Kavan, L. EPR study of ^{17}O-enriched titania nanopowders under UV irradiation. *Catal. Today* **2014**, *230*, 112–118.

53. Finkelstein, E.; Rosen, G.M.; Rauckman, E.J. Production of hydroxyl radical by decomposition of superoxide spin-trapped adducts. *Mol. Pharmacol.* **1982**, *21*, 262–265.
54. Buxton, G.; Greenstock, C.; Helman, W.; Ross, A. Critical-review of rate constants for reactions of hydrated electrons, hydrogen-atoms and hydroxyl radicals ($^{\bullet}OH/^{\bullet}O^{-}$) in aqueous-solution. *J. Phys. Chem. Ref. Data* **1988**, *17*, 513–886.
55. Wilkinson, F.; Helman, W.; Ross, A. Rate constants for the decay and reactions of the lowest electronically excited singlet-state of molecular-oxygen in solution—An expanded and revised compilation. *J. Phys. Chem. Ref. Data* **1995**, *24*, 663–1021.
56. Zalibera, M.; Rapta, P.; Staško, A.; Brindzová, L.; Brezová, V. Thermal generation of stable $SO_4^{\bullet-}$ spin trap adducts with super-hyperfine structure in their EPR spectra: An alternative EPR spin trapping assay for radical scavenging capacity determination in dimethylsulphoxide. *Free Radic. Res.* **2009**, *43*, 457–469.
57. Mottley, C.; Connor, H.D.; Mason, R.P. [^{17}O]oxygen hyperfine structure for the hydroxyl and superoxide radical adducts of the spin traps DMPO, PBN and 4-POBN. *Biochem. Biophys. Res. Commun.* **1986**, *141*, 622–628.
58. Stolze, K.; Rohr-Udilova, N.; Rosenau, T.; Hofinger, A.; Kolarich, D.; Nohl, H. Spin trapping of C- and O-centered radicals with methyl-, ethyl-, pentyl-, and phenyl-substituted EMPO derivatives. *Bioorg. Med. Chem.* **2006**, *14*, 3368–3376.
59. Culcasi, M.; Rockenbauer, A.; Mercier, A.; Clément, J.L.; Pietri, S. The line asymmetry of electron spin resonance spectra as a tool to determine the *cis*:*trans* ratio for spin-trapping adducts of chiral pyrrolines *N*-oxides: The mechanism of formation of hydroxyl radical adducts of EMPO, DEPMPO, and DIPPMPO in the ischemic-reperfused rat liver. *Free Radic. Biol. Med.* **2006**, *40*, 1524–1538.
60. Chalier, F.; Tordo, P. 5-Diisopropoxyphosphoryl-5-methyl-1-pyrroline *N*-oxide, DIPPMPO, a crystalline analog of the nitrone DEPMPO: Synthesis and spin trapping properties. *J. Chem. Soc. Perkin Trans. 2* **2002**, 2110–2117, doi:10.1039/B206909C.
61. Huling, S.G.; Arnold, R.G.; Sierka, R.A.; Miller, M.R. Measurement of hydroxyl radical activity in a soil slurry using the spin trap α-(4-pyridyl-1-oxide)-*N*-*tert*-butylnitrone. *Environ. Sci. Technol.* **1998**, *32*, 3436–3441.
62. Brezová, V.; Tarábek, P.; Dvoranová, D.; Staško, A.; Biskupič, S. EPR study of photoinduced reduction of nitroso compounds in titanium dioxide suspensions. *J. Photochem. Photobiol. A Chem.* **2003**, *155*, 179–198.
63. Clement, J.; Gilbert, B.; Ho, W.; Jackson, N.; Newton, M.; Silvester, S.; Timmins, G.; Tordo, P.; Whitwood, A. Use of a phosphorylated spin trap to discriminate between the hydroxyl radical and other oxidising species. *J. Chem. Soc. Perkin Trans. 2* **1998**, 1715–1718, doi:10.1039/A804098B.
64. Patel, A.; Rohr-Udilova, N.; Rosenau, T.; Stolze, K. Synthesis and characterization of 5-alkoxycarbonyl-4-hydroxymethyl-5-alkyl-pyrroline *N*-oxide derivatives. *Bioorg. Med. Chem.* **2011**, *19*, 7643–7652.
65. Stolze, K.; Rohr-Udilova, N.; Hofinger, A.; Rosenau, T. Spin trapping properties of aminocarbonyl- and methylamino-carbonyl-substituted EMPO derivatives. *Free Radic. Res.* **2009**, *43*, 81–81.

66. Abbas, K.; Hardy, M.; Poulhès, F.; Karoui, H.; Tordo, P.; Ouari, O.; Peyrot, F. Detection of superoxide production in stimulated and unstimulated living cells using new cyclic nitrone spin traps. *Free Radic. Biol. Med.* **2014**, *71*, 281–290.
67. Halliwel, B.; Gutteridge, J. *Free Radicals in Biology and Medicine*, 3rd ed.; Oxford University Press: Oxford, UK, 1999; p. 60.
68. Hirakawa, T.; Nakaoka, Y.; Nishino, J.; Nosaka, Y. Primary passages for various TiO_2 photocatalysts studied by means of luminol chemiluminescent probe. *J. Phys. Chem. B* **1999**, *103*, 4399–4403.
69. Nosaka, Y.; Yamashita, Y.; Fukuyama, H. Application of chemiluminescent probe to monitoring superoxide radicals and hydrogen peroxide in TiO_2 photocatalysis. *J. Phys. Chem. B* **1997**, *101*, 5822–5827.
70. Nosaka, Y.; Fukuyama, H. Application of chemiluminescent probe to the characterization of TiO_2 photocatalysts in aqueous suspension. *Chem. Lett.* **1997**, *26*, 383–384.
71. Marino, T.; Molinari, R.; García, H. Selectivity of gold nanoparticles on the photocatalytic activity of TiO_2 for the hydroxylation of benzene by water. *Catal. Today* **2013**, *206*, 40–45.
72. Molinari, A.; Maldotti, A.; Amadelli, R. Probing the role of surface energetics of electrons and their accumulation in photoreduction processes on TiO_2. *Chem. Eur. J.* **2014**, *20*, 7759–7765.
73. Brezová, V.; Gabčová, S.; Dvoranová, D.; Staško, A. Reactive oxygen species produced upon photoexcitation of sunscreens containing titanium dioxide (An EPR study). *J. Photochem. Photobiol. B Biol.* **2005**, *79*, 121–134.
74. Barbieriková, Z.; Mihalíková, M.; Brezová, V. Photoinduced oxidation of sterically hindered amines in acetonitrile solutions and titania suspensions (An EPR study). *Photochem. Photobiol.* **2012**, *88*, 1442–1454.
75. Lide, D.R., Ed. *CRC Handbook of Chemistry and Physics*, 86th ed.; CRC Press: Boca Raton, FL, USA, 2005.
76. Mitroka, S.; Zimmeck, S.; Troya, D.; Tanko, J. How solvent modulates hydroxyl radical reactivity in hydrogen atom abstractions. *J. Am. Chem. Soc.* **2010**, *132*, 2907–2913.
77. Turro, N.J.; Ramamurthy, V.; Scaiano, J.C. *Modern Molecular Photochemistry of Organic Molecules*; University Science Books: Sausalito, CA, USA, 2010; p. 1008.
78. Wadhawan, J.; Welford, P.; McPeak, H.; Hahn, C.; Compton, R. The simultaneous voltammetric determination and detection of oxygen and carbon dioxide—A study of the kinetics of the reaction between superoxide and carbon dioxide in non-aqueous media using membrane-free gold disc microelectrodes. *Sens. Actuat. B* **2003**, *88*, 40–52.
79. Golovanov, I.; Zhenodarova, S. Quantitative structure-property relationship: XXIII. Solubility of oxygen in organic solvents. *Russ. J. Gen. Chem.* **2005**, *75*, 1795–1797.
80. Di Paola, A.; Bellardita, M.; Palmisano, L.; Barbieriková, Z.; Brezová, V. Influence of crystallinity and OH surface density on the photocatalytic activity of TiO_2 powders. *J. Photochem. Photobiol. A Chem.* **2014**, *273*, 59–67.
81. Addamo, M.; Augugliaro, V.; Coluccia, S.; di Paola, A.; García-López, E.; Loddo, V.; Marcì, G.; Martra, G.; Palmisano, L. The role of water in the photocatalytic degradation of acetonitrile and toluene in gas-solid and liquid-solid regimes. *Int. J. Photoenergy* **2006**, *2006*, doi:10.1155/IJP/2006/39182.

82. Micic, O.; Zhang, Y.; Cromack, K.; Trifunac, A.; Thurnauer, M. Photoinduced hole transfer from TiO_2 to methanol molecules in aqueous-solution studied by electron-paramagnetic-resonance. *J. Phys. Chem.* **1993**, *97*, 13284–13288.
83. Pieta, P.; Petr, A.; Kutner, W.; Dunsch, L. *In situ* ESR spectroscopic evidence of the spin-trapped superoxide radical, $O_2^{\bullet-}$, electrochemically generated in DMSO at room temperature. *Electrochim. Acta* **2008**, *53*, 3412–3415.
84. Barbieriková, Z.; Bella, M.; Kučerák, J.; Milata, V.; Jantová, S.; Dvoranová, D.; Veselá, M.; Staško, A.; Brezová, V. Photoinduced superoxide radical anion and singlet oxygen generation in the presence of novel selenadiazoloquinolones (An EPR study). *Photochem. Photobiol.* **2011**, *87*, 32–44.
85. Guo, R.; Davies, C.; Nielsen, B.; Hamilton, L.; Symons, M.; Winyard, P. Reaction of the spin trap 3,5-dibromo-4-nitrosobenzene sulfonate with human biofluids. *Biochim. Biophys. Acta Gen. Subj.* **2002**, *1572*, 133–142.
86. Konaka, R.; Terabe, S.; Mizuta, T.; Sakata, S. Spin trapping by use of nitrosodurene and its derivatives. *Can. J. Chem.* **1982**, *60*, 1532–1542.
87. Terabe, S.; Kuruma, K.; Konaka, R. Spin trapping by use of nitroso-compounds. Part VI. Nitrosodurene and other nitrosobenzene derivatives. *J. Chem. Soc.***1973**, *9*, 1252–1258.
88. Daimon, T.; Hirakawa, T.; Nosaka, Y. Monitoring the formation and decay of singlet molecular oxygen in TiO_2 photocatalytic systems and the reaction with organic molecules. *Electrochemistry* **2008**, *76*, 136–139.
89. Daimon, T.; Nosaka, Y. Formation and behavior of singlet molecular oxygen in TiO_2 photocatalysis studied by detection of near-infrared phosphorescence. *J. Phys. Chem. C* **2007**, *111*, 4420–4424.
90. Daimon, T.; Hirakawa, T.; Kitazawa, M.; Suetake, J.; Nosaka, Y. Formation of singlet molecular oxygen associated with the formation of superoxide radicals in aqueous suspensions of TiO_2 photocatalysts. *Appl. Catal. A* **2008**, *340*, 169–175.
91. Nakamura, K.; Ishiyama, K.; Ikai, H.; Kanno, T.; Sasaki, K.; Niwano, Y.; Kohno, M. Reevaluation of analytical methods for photogenerated singlet oxygen. *J. Clin. Biochem. Nutr.* **2011**, *49*, 87–95.
92. Wu, H.; Song, Q.; Ran, G.; Lu, X.; Xu, B. Recent developments in the detection of singlet oxygen with molecular spectroscopic methods. *TrAC Trends Anal. Chem.* **2011**, *30*, 133–141.
93. Barbieriková, Z.; Bella, M.; Sekeráková, L.; Lietava, J.; Bobeničová, M.; Dvoranová, D.; Milata, V.; Sádecká, J.; Topoľská, D.; Heizer, T.; *et al*. Spectroscopic characterization, photoinduced processes and cytotoxic properties of substituted *N*-ethyl selenadiazoloquinolones. *J. Phys. Org. Chem.* **2013**, *26*, 565–574.
94. Lion, Y.; Gandin, E.; van de Vorst, A. On the production of nitroxide radicals by singlet oxygen reaction: An EPR study. *Photochem. Photobiol.* **1980**, *31*, 305–309.
95. Nosaka, Y.; Natsui, H.; Sasagawa, M.; Nosaka, A. Electron spin resonance studies on the oxidation mechanism of sterically hindered cyclic amines in TiO_2 photocatalytic systems. *J. Phys. Chem. B* **2006**, *110*, 12993–12999.
96. Maldotti, A.; Amadelli, R.; Carassiti, V. An electron spin resonance spin trapping investigation of azide oxidation on TiO_2 powder suspensions. *Can. J. Chem.* **1988**, *66*, 76–80.

97. Konovalova, T.A.; Lawrence, J.; Kispert, L.D. Generation of superoxide anion and most likely singlet oxygen in irradiated TiO_2 nanoparticles modified by carotenoids. *J. Photochem. Photobiol. A Chem.* **2004**, *162*, 1–8.
98. Jomová, K.; Valko, M. Health protective effects of carotenoids and their interactions with other biological antioxidants. *Eur. J. Med. Chem.* **2013**, *70*, 102–110.
99. Duling, D.R. Simulation of multiple isotropic spin-trap EPR spectra. *J. Magn. Reson. B* **1994**, *104*, 105–110. Available online: http://www.niehs.nih.gov/research/resources/software/tox-pharm/tools/ (accessed on 22 October 2014).

Sample Availability: Not available.